

# Effects of the Addition of Copper Chloride and Potassium Iodide to Methylammonium-Based Perovskite Solar Cells <sup>†</sup>

Ayu Enomoto <sup>1</sup>, Atsushi Suzuki <sup>1,\*</sup> , Takeo Oku <sup>1</sup> , Masanobu Okita <sup>2</sup>, Sakiko Fukunishi <sup>2</sup>, Tomoharu Tachikawa <sup>2</sup> and Tomoya Hasegawa <sup>2</sup>

<sup>1</sup> Department of Materials Science, The University of Shiga Prefecture, 2500 Hassaka, Hikone 522-8533, Shiga, Japan

<sup>2</sup> Osaka Gas Chemicals Co., Ltd., 5-11-61 Torishima, Konohana-ku, Osaka 554-0051, Osaka, Japan

\* Correspondence: [suzuki@mat.usp.ac.jp](mailto:suzuki@mat.usp.ac.jp); Tel.: +81-749-28-8369

<sup>†</sup> Presented at the 3rd International Electronic Conference on Applied Sciences, 1–15 December 2022; Available online: <https://asec2022.sciforum.net/>.

**Abstract:** Organic–inorganic hybrid perovskite solar cells have the advantage of being able to implement a high conversion efficiency, easy fabrication process and low cost to commercial products of photovoltaic devices. The perovskite solar cells have a photovoltaic performance with reduced durability due to the volatility of organic cations and toxic lead in the perovskite crystal as an active layer. The purpose of this research is to investigate the effect of additives such as copper chloride and potassium iodide in the perovskite crystal on the photovoltaic properties and electronic structure. The distribution of 3d orbital of copper ion conjugated with 5p orbital of iodine ion at the valence band, and 6p orbital of lead ion at the conduction band, influences the charge generation and transfer, as well as the carrier mobility with a narrowing band gap. The addition of potassium iodide delocalizes the charge distribution near the copper, iodide, and lead ions, which promotes the charge generation and carrier diffusion, yielding an increase in the short circuit current density relating to the conversion efficiency.

**Keywords:** perovskite; solar cell; photovoltaic device; copper; methylammonium; potassium; polysilane; decaphenylcyclopentasilane



**Citation:** Enomoto, A.; Suzuki, A.; Oku, T.; Okita, M.; Fukunishi, S.; Tachikawa, T.; Hasegawa, T.

Effects of the Addition of Copper Chloride and Potassium Iodide to Methylammonium-Based Perovskite Solar Cells. *Eng. Proc.* **2023**, *31*, 31.

<https://doi.org/10.3390/ASEC2022-13885>

Academic Editor: Nunzio Cennamo

Published: 21 December 2022



**Copyright:** © 2022 by the authors. Licensee MDPI, Basel, Switzerland. This article is an open access article distributed under the terms and conditions of the Creative Commons Attribution (CC BY) license (<https://creativecommons.org/licenses/by/4.0/>).

## 1. Introduction

Lead halide perovskite semiconductors attracted attention as the active layer of electroluminescence in the 1990s [1]. After the first application of a  $\text{CH}_3\text{NH}_3\text{PbI}_3$  compound to solar cells [2], the lead halide perovskites have been actively researched worldwide [3–7]. Since  $\text{CH}_3\text{NH}_3\text{PbI}_3$  perovskite solar cells have a high sensitivity to visible light and an easy production process, it is expected that they will be next-generation solar cells. However, toxicity problems in including Pb perovskite solar cells have impeded their wholesale commercial application. Moreover, the long-term instability caused by the decomposition of perovskite crystal has still not been resolved. The contamination of soil and water by  $\text{Pb}^{2+}$  ions is permanent. When organisms take in Pb, it is not eliminated from the body and causes serious adverse effects. It enters the human body and causes dysfunction in the nervous, digestive, and blood systems. It is mandatory to provide safe and environmentally friendly products. From previous studies, less toxic ions such as  $\text{Sn}^{2+}$ ,  $\text{Ge}^{2+}$ ,  $\text{Co}^{2+}$ , and  $\text{Cu}^{2+}$  are expected to be alternative elements [8–12]. Among them, the environmentally friendly transition metal  $\text{Cu}^{2+}$  has been examined as a candidate for  $\text{Pb}^{2+}$  replacement, but there are few reported cases [13–15]. In addition, the durability of perovskite solar cell is caused mainly by the decomposition of the perovskite crystals due to methylammonium (MA) desorption. To solve these problems, attempts to introduce additives into the perovskite layer to improve the electronic properties have been studied [16–27]. Previous studies have reported that the substitution of potassium (K) can inhibit MA desorption,

resulting in improved performance and long-term stability [28–33]. The aim of this work is to fabricate and characterize the perovskite solar cell doped with copper chloride and potassium iodide. The photovoltaic properties, morphologies, and crystal structure were investigated via the substitution of  $\text{Cu}^{2+}$  and  $\text{K}^+$  ions. The stability of the performance was measured. In addition, first-principle calculations were performed and compared with the experimental results.

## 2. Materials and Methods

The present perovskite solar cells were prepared according to the literature [34–38]. For preparing the perovskite compound, a mixture of  $\text{CH}_3\text{NH}_3\text{I}$  (MAI, Tokyo Chemical Industry, 2.4 M),  $\text{PbCl}_2$  (0.8 M, Sigma-Aldrich, Tokyo, Japan), copper chloride ( $\text{CuCl}_2$ , Sigma Aldrich), and potassium iodide (KI, Wako Pure Chemical Corporation, Osaka, Japan) with the desired molar ratio in *N,N*-dimethylformamide (DMF, NacalaiTesque, Kyoto, Japan, 0.5 mL), was stirred at 60 °C for 24 h. As a standard recipe, the mole of MAI and  $\text{PbCl}_2$  in DMF was adjusted to be 2.4 M (190.8 mg) and 0.8 M (111.2 mg). In the doped case of 2%  $\text{CuCl}_2$ , the mole of MAI,  $\text{PbCl}_2$ , and  $\text{CuCl}_2$  was adjusted to be 2.4 M (190.8 mg), 0.78 M (109.0 mg), and 0.02 M (1.07 mg). In the doped case of 2%  $\text{CuCl}_2$  and 2% KI, the mole of MAI,  $\text{PbCl}_2$ , KI, and  $\text{CuCl}_2$  was adjusted to be 2.35 M (186.9 mg), 0.78 M (109 mg), 0.01 M (0.93 mg), and 0.02 M (1.07 mg). The perovskite solutions were spin-coated on  $\text{TiO}_2$  with air flow at three times. A solution of decaphenylcyclopentasilane (DPPS, Osaka Gas Chemical, OGSOL SI-30-15, 10 mg) was prepared in chlorobenzene (0.5 mL) and dropped onto the perovskite layer during the last stage of the spin-coating process. DPPS was used as a hole-transporting material, with the cell being protected from moisture and oxygen. Annealing process was performed at 200 °C. All procedures were performed in air atmosphere. A gold (Au) electrode was deposited to serve as the top electrode. The structure of the solar cells is denoted as  $\text{FTO}/\text{TiO}_2/\text{perovskite}/\text{DPPS}/\text{spiro-OMeTAD}/\text{Au}$ . The prepared cells were stored at temperature of 22 °C and with humidity below 30%.

The electronic structures of the Cu-, and K-doped perovskite crystal were single-point and calculated using ab initio quantum calculation [39–45] based on the restricted Hartree–Fock method and hybrid density functional theory (DFT) using restricted B3LYP with LANL2MB as the basis set (Gaussian 09). The  $\text{MAPbI}_3$  perovskite crystals with supercells of  $2 \times 2 \times 2$  as cluster model were formed on the basis of the experimental results using X-ray diffraction data.

## 3. Results and Discussion

### 3.1. First-Principles Calculation

Electron density distributions at the highest occupied molecular orbital (HOMO) and lowest unoccupied molecular orbital (LUMO) as well as the electrostatic potential (ESP) and partial charge of  $\text{MAPb}(\text{Cu})\text{I}_3$  and  $\text{MA}(\text{K})\text{Pb}(\text{Cu})\text{I}_3$  perovskite cubic crystals with  $2 \times 2 \times 2$  supercells are shown in Figure 1a,b, respectively. The electron density distributions of the  $\text{MAPb}(\text{Cu})\text{I}_3$  perovskite demonstrated that the 6p orbitals of the Pb atom dominated at the LUMO. The 3d orbitals of  $\text{Cu}^{2+}$  ion and the 5p orbitals of the  $\text{I}^-$  ion were delocalized at the HOMO. The charge transfer between the 3d orbitals of the  $\text{Cu}^{2+}$  ion and the 5p orbital of the  $\text{I}^-$  ion would promote the carrier generation and carrier diffusion.

The electron density distributions of the  $\text{MA}(\text{K})\text{Pb}(\text{Cu})\text{I}_3$  perovskite are shown in Figure 1b. The 6p orbitals of the  $\text{Pb}^{2+}$  ion and the 4s orbitals of the  $\text{Cu}^{2+}$  ion were formed in the LUMO. The 3d orbitals of the  $\text{Cu}^{2+}$  ion and the 5p orbitals of the  $\text{I}^-$  ion were dominated in the HOMO. The addition of  $\text{K}^+$  caused 4s orbitals of  $\text{Cu}^{2+}$  conjugated with 6p orbital of Pb ion in the LUMO, promoting charge transfer between 4s orbital and 6p orbital in the coordination band. For the ESP and partial charge of  $\text{MAPb}(\text{Cu})\text{I}_3$  and  $\text{MA}(\text{K})\text{Pb}(\text{Cu})\text{I}_3$  perovskite, the charges of  $\text{Cu}^{2+}$  and  $\text{I}^-$  ion were delocalized by the positive charge of  $\text{K}^+$ , which would promote the carrier diffusion and an increase in short circuit current density.

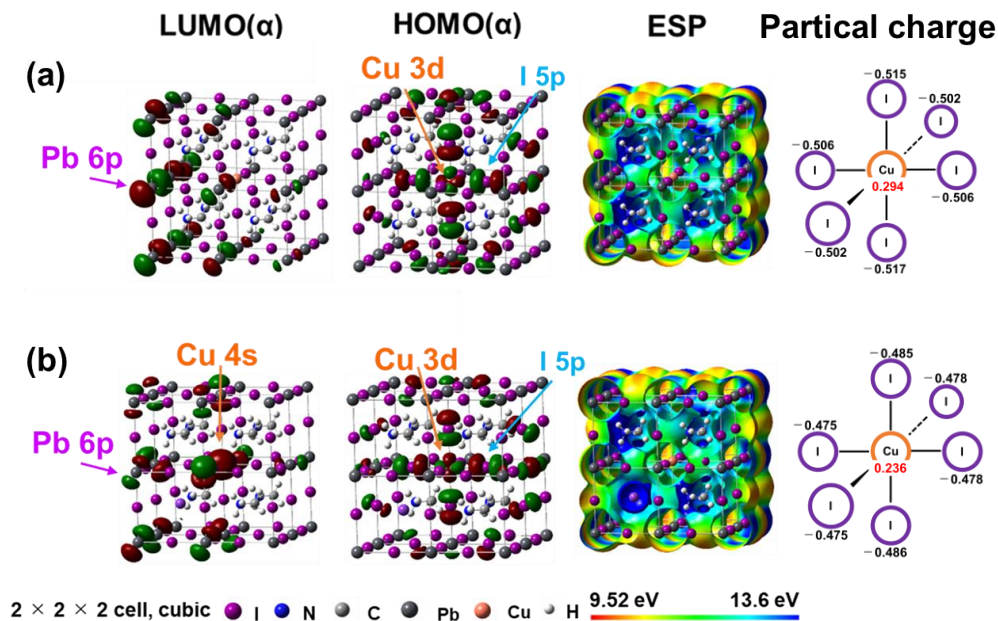


**Figure 1.** The electron density distributions at the highest occupied molecular orbital (HOMO) and lowest unoccupied molecular orbital (LUMO), electrostatic potential (ESP) and partial charge of (a)  $\text{MAPb}_{0.963}\text{Cu}_{0.037}\text{I}_3$  and (b)  $\text{MA}_{0.875}\text{K}_{0.125}\text{Pb}_{0.963}\text{Cu}_{0.037}\text{I}_3$  perovskite cubic crystals with  $2 \times 2 \times 2$  supercells.

### 3.2. Device Characterization

The photovoltaic parameters of open-circuit voltage ( $V_{\text{OC}}$ ), short-circuit current density ( $J_{\text{SC}}$ ), fill factor (FF), conversion efficiency ( $\eta$ ), and band gap ( $E_{\text{g}}$ ) are listed in Table 1. The conversion efficiencies of the Cu- and K-doped perovskite solar cells were found to be 10.59%, which were higher than that of the Cu-added solar cell. The addition of  $\text{Cu}^{2+}$  and  $\text{K}^{+}$  ions supported the photovoltaic performance with an increase in  $J_{\text{SC}}$  related to  $\eta$ , due to the enhancement of the carrier transfer in the perovskite crystal.

**Table 1.** Photovoltaic parameters of present perovskite photovoltaic devices.

Devices	$J_{\text{SC}}$ ( $\text{mA cm}^{-2}$ )	$V_{\text{OC}}$ (V)	FF	$\eta$ (%)	$\eta_{\text{ave}}$ (%)	$E_{\text{g}}$ (eV)
$\text{MAPbI}_3$	21.6	0.822	0.622	11.03	9.00	1.56
+ $\text{Cu}^{2+}$ 2%	18.5	0.800	0.627	9.26	8.47	1.56
+ $\text{Cu}^{2+}$ 2%, $\text{K}^{+}$ 2%	21.4	0.837	0.590	10.59	8.99	1.56

## 4. Conclusions

The fabrication and characterization of Cu- and K-doped  $\text{MAPbI}_3$  perovskite solar cells was performed. The photovoltaic properties and electronic structures were investigated. The 2% Cu- and 2% K-doped perovskite solar cells had the photovoltaic performance of conversion efficiency with increases in the  $J_{\text{sc}}$  values. The charge transfer between the 3d orbital of the  $\text{Cu}^{2+}$  ion and the 5p orbitals of the  $\text{I}^{-}$  ion would influence the carrier generation and diffusion in the cubic  $\text{MAPb}(\text{Cu})\text{I}_3$  perovskite. Addition of  $\text{K}^{+}$  into  $\text{MAPb}(\text{Cu})\text{I}_3$  perovskite caused the 3d orbital of the  $\text{Cu}^{2+}$  ion in the HOMO and LUMO. The addition of  $\text{K}^{+}$  delocalized the 3d and 5p orbitals of the  $\text{Cu}^{2+}$  and  $\text{I}^{-}$  ions near the HOMO as well as the 4s and 6p orbital of the  $\text{Cu}^{2+}$  and  $\text{Pb}^{2+}$  ions near the LUMO with a wide charge distribution, which promoted the carrier generation and charge transfer, yielding an increase in  $J_{\text{SC}}$  related to  $\eta$ .

**Author Contributions:** Conceptualization, A.E., A.S. and T.O.; methodology, A.E., A.S. and T.O.; formal analysis, A.E. and A.S.; investigation, A.E.; resources, A.S., T.O., M.O., S.F., T.T. and T.H.; data curation, A.E. and A.S.; writing—original draft preparation, A.E., A.S. and T.O.; project administration, A.S. and T.O.; funding acquisition, A.S. and T.O. All authors have read and agreed to the published version of the manuscript.

**Funding:** This research was supported by JSPS KAKENHI Grant Number JP 21K05261.

**Institutional Review Board Statement:** Not applicable.

**Informed Consent Statement:** Not applicable.

**Data Availability Statement:** Data is contained within the article.

**Conflicts of Interest:** The authors declare no conflict of interest.

## References

- Chondroudis, K.; Mitzi, D.B. Electroluminescence from an organic–inorganic perovskite incorporating a quaterthiophene dye within lead halide perovskite layers. *Chem. Mater.* **1999**, *11*, 3028. [\[CrossRef\]](#)
- Kojima, A.; Teshima, K.; Shirai, Y.; Miyasaka, T. Organometal halide perovskites as visible-light sensitizers for photovoltaic cells. *J. Am. Chem. Soc.* **2009**, *131*, 6050. [\[CrossRef\]](#)
- Kovalenko, M.V.; Protesescu, L.; Bodnarchuk, M.I. Properties and potential optoelectronic applications of lead halide perovskite nanocrystals. *Science* **2017**, *358*, 745–750. [\[CrossRef\]](#)
- Wang, D.; Wright, M.; Elumalai, N.K.; Uddin, A. Stability of perovskite solar cells. *Sol. Energy Mater. Sol. Cells* **2016**, *147*, 255. [\[CrossRef\]](#)
- Chen, S.; Dai, X.; Xu, S.; Jiao, H.; Zhao, L.; Huang, J. Stabilizing perovskite-substrate interfaces for high-performance perovskite modules. *Science* **2021**, *373*, 902. [\[CrossRef\]](#) [\[PubMed\]](#)
- Zou, Y.; Teng, P.; Xu, W.; Zheng, G.; Lin, W.; Yin, J.; Kobera, L.; Abbrent, S.; Li, X.; Steele, J.A.; et al. Manipulating crystallization dynamics through chelating molecules for bright perovskite emitters. *Nat. Commun.* **2021**, *12*, 4831. [\[CrossRef\]](#)
- Wang, Y.; Mahmoudi, T.; Hahn, Y. Highly stable and efficient perovskite solar cells based on FAMA-perovskite-Cu:NiO composites with 20.7% efficiency and 80.5% fill factor. *Adv. Energy Mater.* **2020**, *10*, 27. [\[CrossRef\]](#)
- Noel, N.K.; Stranks, S.D.; Abate, A.; Wehrenfennig, C.; Guarnera, S.; Haghighirad, A.A.; Sadhanala, A.; Eperon, G.E.; Pathak, S.K.; Johnston, M.B.; et al. Lead-free organic-inorganic tin halide perovskites for photovoltaic applications. *Energy Environ. Sci.* **2014**, *9*, 3061–3068. [\[CrossRef\]](#)
- Krishnamoorthy, T.; Ding, H.; Yan, C.; Leong, W.L.; Baikie, T.; Zhang, Z.; Sherburne, M.; Li, S.; Asta, M.; Mathews, N.; et al. Lead-free germanium iodide perovskite materials for photovoltaic applications. *J. Mater. Chem. A* **2015**, *47*, 23829–23832. [\[CrossRef\]](#)
- Shao, S.; Liu, J.; Portale, G.; Fang, H.-H.; Blake, G.R.; Brink, G.H.t.; Koster, L.J.A.; Loi, M.A. Highly reproducible Sn-based hybrid perovskite solar cells with 9% efficiency. *Adv. Energy Mater.* **2018**, *8*, 1702019. [\[CrossRef\]](#)
- Wang, P.; Chen, B.; Li, R.; Wang, S.; Ren, N.; Li, Y.; Mazumdar, S.; Shi, B.; Zhao, Y.; Zhang, X. Cobalt Chloride Hexahydrate Assisted in Reducing Energy Loss in Perovskite Solar Cells with Record Open-Circuit Voltage of 1.20 V. *ACS Energy Lett.* **2021**, *6*, 2121–2128. [\[CrossRef\]](#)
- Suzuki, A.; Oe, M.; Oku, T. Fabrication and characterization of Ni-, Co-, and Rb-incorporated CH<sub>3</sub>NH<sub>3</sub>PbI<sub>3</sub> perovskite solar cells. *J. Electron. Mater.* **2021**, *50*, 1980–1995. [\[CrossRef\]](#)
- Ueoka, N.; Oku, T.; Suzuki, A. Effects of doping with Na, K, Rb, and formamidinium cations on (CH<sub>3</sub>NH<sub>3</sub>)<sub>0.99</sub>Rb<sub>0.01</sub>Pb<sub>0.99</sub>Cu<sub>0.01</sub>I<sub>3-x</sub>(Cl,Br)<sub>x</sub> perovskite photovoltaic cells. *AIP Adv.* **2020**, *10*, 125023. [\[CrossRef\]](#)
- Ge, X.; Qu, X.; He, L.; Sun, Y.; Guan, X.; Pang, Z.; Wang, C.; Yang, L.; Wang, F.; Rosei, F. 3D low toxicity Cu–Pb binary perovskite films and their photoluminescent/photovoltaic performance. *J. Mater. Chem. A* **2019**, *7*, 27225–27235. [\[CrossRef\]](#)
- Ueoka, N.; Oku, T. Effects of co-addition of sodium chloride and copper (II) bromide to mixed-cation mixed-halide perovskite photovoltaic devices. *ACS Appl. Energy Mater.* **2020**, *3*, 7272–7283. [\[CrossRef\]](#)
- Oku, T. Crystal structures of perovskite halide compounds used for solar cells. *Rev. Adv. Mater. Sci.* **2020**, *59*, 264–305. [\[CrossRef\]](#)
- Wu, C.; Chen, K.; Guo, D.Y.; Wang, S.L.; Li, P.G. Cations substitution tuning phase stability in hybrid perovskite single crystals by strain relaxation. *RSC Adv.* **2018**, *8*, 2900–2905. [\[CrossRef\]](#) [\[PubMed\]](#)
- Tavakoli, M.M.; Zakeeruddin, S.M.; Grätzel, M.; Fan, Z. Large-grain tin-rich perovskite films for efficient solar cells via metal alloying technique. *Adv. Mater.* **2018**, *30*, 11. [\[CrossRef\]](#)
- Oku, T.; Ohishi, Y.; Suzuki, A. Effects of antimony addition to perovskite-type CH<sub>3</sub>NH<sub>3</sub>PbI<sub>3</sub> photovoltaic devices. *Chem. Lett.* **2016**, *45*, 134. [\[CrossRef\]](#)
- Li, M.; Wang, Z.K.; Zhuo, M.P.; Hu, Y.; Hu, K.H.; Ye, Q.Q.; Jain, S.M.; Yang, Y.G.; Gao, X.Y.; Liao, L.S. Pb–Sn–Cu ternary organometallic halide perovskite solar cells. *Adv. Mater.* **2018**, *30*, 1800258. [\[CrossRef\]](#)
- Khalid, M.; Roy, A.; Bhandari, S.; Selvaraj, P.; Sundaram, S.; Mallick, T.K. Opportunities of copper addition in CH<sub>3</sub>NH<sub>3</sub>PbI<sub>3</sub> perovskite and their photovoltaic performance evaluation. *J. Alloys Compd.* **2022**, *895*, 162626. [\[CrossRef\]](#)



22. Elseman, A.M.; Shalan, A.E.; Sajid, S.; Rashad, M.M.; Hassan, A.M.; Li, M. Copper-substituted lead perovskite materials constructed with different halides for working  $(\text{CH}_3\text{NH}_3)_2\text{CuX}_4$ -based perovskite solar cells from experimental and theoretical view. *ACS Appl. Mater. Interfaces* **2018**, *10*, 11699–11707. [[CrossRef](#)]
23. Tanaka, H.; Ohishi, Y.; Oku, T. Fabrication and characterization of the copper bromides-added  $\text{CH}_3\text{NH}_3\text{PbI}_{3-x}\text{Cl}_x$  perovskite solar cells. *Synth. Met.* **2018**, *244*, 128. [[CrossRef](#)]
24. Ueoka, N.; Oku, T.; Suzuki, A. Additive effects of alkali metals on Cu-modified  $\text{CH}_3\text{NH}_3\text{PbI}_{3-\delta}\text{Cl}_\delta$  photovoltaic devices. *RSC Adv.* **2019**, *9*, 24231. [[CrossRef](#)] [[PubMed](#)]
25. Li, Y.; Zhou, Z.; Tewari, N.; Ng, M.; Geng, P.; Chen, D.; Ko, P.K.; Qammar, M.; Guo, L.; Halpert, J.E. Progress in copper metal halides for optoelectronic applications. *Mater. Chem. Front.* **2021**, *5*, 4796–4820. [[CrossRef](#)]
26. Karthick, S.; Hawashin, H.; Parou, N.; Vedraïne, S.; Velumani, S.; Boucle, J. Copper and bismuth incorporated mixed cation perovskite solar cells by one-step solution process. *Sol. Energy* **2021**, *218*, 226. [[CrossRef](#)]
27. Wang, K.-L.; Wang, R.; Wang, Z.K.; Li, M.; Zhang, Y.; Ma, H.; Liao, L.-S.; Yang, Y. Tailored phase transformation of  $\text{CsPbI}_2\text{Br}$  films by copper(II) bromide for high-performance all-inorganic perovskite solar cells. *Nano Lett.* **2019**, *19*, 5176–5184. [[CrossRef](#)] [[PubMed](#)]
28. Tang, Z.; Bessho, T.; Awai, F.; Kinoshita, T.; Maitani, M.; Jono, R.; Murakami, T.N.; Wang, H.; Kubo, T.; Uchida, S.; et al. Hysteresis-free perovskite solar cells made of potassium-doped organometal halide perovskite. *Sci. Rep.* **2017**, *7*, 12183. [[CrossRef](#)]
29. Alanazi, T.I.; Game, O.S.; Smith, J.A.; Kilbride, R.C.; Greenland, C.; Jayaprakash, R.; Georgiou, K.; Terrill, N.J.; Lidzey, D.G. Potassium iodide reduces the stability of triple-cation perovskite solar cells. *RSC Adv.* **2020**, *10*, 40341–40350. [[CrossRef](#)] [[PubMed](#)]
30. Kandori, S.; Oku, T.; Nishi, K.; Kishimoto, T.; Ueoka, N.; Suzuki, A. Fabrication and characterization of potassium- and formamidinium-added perovskite solar cells. *J. Ceram. Soc. Jpn.* **2020**, *128*, 805–811. [[CrossRef](#)]
31. Jiang, J.; Xu, J.; Walter, H.; Kazi, A.; Wang, D.; Wangila, G.; Mortazavi, M.; Yan, C.; Jiang, Q. The doping of alkali metal for halide perovskites. *ES Mater. Manuf.* **2020**, *7*, 25–33. [[CrossRef](#)]
32. Oku, T.; Zushi, M.; Imanishi, Y.; Suzuki, A.; Suzuki, K. Microstructures and photovoltaic properties of perovskite-type  $\text{CH}_3\text{NH}_3\text{PbI}_3$  compounds. *Appl. Phys. Express* **2014**, *7*, 121601. [[CrossRef](#)]
33. Machiba, H.; Oku, T.; Kishimoto, T.; Ueoka, N.; Suzuki, A. Fabrication and evaluation of K-doped  $\text{MA}_{0.8}\text{FA}_{0.1}\text{K}_{0.1}\text{PbI}_3(\text{Cl})$  perovskite solar cells. *Chem. Phys. Lett.* **2019**, *730*, 117. [[CrossRef](#)]
34. Oku, T.; Ohishi, Y.; Ueoka, N. Highly (100)-oriented  $\text{CH}_3\text{NH}_3\text{PbI}_3(\text{Cl})$  perovskite solar cells prepared with  $\text{NH}_4\text{Cl}$  using an air blow method. *RSC Adv.* **2018**, *8*, 10389–10395. [[CrossRef](#)]
35. Oku, T.; Kandori, S.; Taguchi, M.; Suzuki, A.; Okita, M.; Minami, S.; Fukunishi, S.; Tachikawa, T. Polysilane-inserted methylammonium lead iodide perovskite solar cells doped with formamidinium and potassium. *Energies* **2020**, *13*, 4776. [[CrossRef](#)]
36. Taguchi, M.; Suzuki, A.; Oku, T.; Ueoka, N.; Minami, S.; Okita, M. Effects of annealing temperature on decaphenylcyclopentasilane-inserted  $\text{CH}_3\text{NH}_3\text{PbI}_3$  perovskite solar cells. *Chem. Phys. Lett.* **2019**, *737*, 136822. [[CrossRef](#)]
37. Oku, T.; Ueoka, N.; Suzuki, K.; Suzuki, A.; Yamada, M.; Sakamoto, H.; Minami, S.; Fukunishi, S.; Kohno, K.; Miyauchi, S. Fabrication and characterization of perovskite photovoltaic devices with  $\text{TiO}_2$  nanoparticle layers. *AIP Conf. Proc.* **2017**, *1807*, 020014. [[CrossRef](#)]
38. Oku, T.; Taguchi, M.; Suzuki, A.; Kitagawa, K.; Asakawa, Y.; Yoshida, S.; Okita, M.; Minami, S.; Fukunishi, S.; Tachikawa, T. Effects of polysilane addition to chlorobenzene and high temperature annealing on  $\text{CH}_3\text{NH}_3\text{PbI}_3$  perovskite photovoltaic devices. *Coatings* **2021**, *11*, 665. [[CrossRef](#)]
39. Suzuki, A.; Oku, T. First-principles calculation study of electronic structures of alkali metals (Li, K, Na and Rb)-incorporated formamidinium lead halide perovskite compounds. *Appl. Surf. Sci.* **2019**, *483*, 912–921. [[CrossRef](#)]
40. Suzuki, A.; Miyamoto, Y.; Oku, T. Electronic structures, spectroscopic properties, and thermodynamic characterization of sodium- or potassium- incorporated  $\text{CH}_3\text{NH}_3\text{PbI}_3$  by first principles calculation. *J. Mater. Sci.* **2020**, *55*, 9728. [[CrossRef](#)]
41. Suzuki, A.; Oku, T. Effects of mixed-valence states of Eu-doped  $\text{FAPbI}_3$  perovskite crystals studied by first-principles calculation. *Mater. Adv.* **2021**, *2*, 2609–2616. [[CrossRef](#)]
42. Ono, I.; Oku, T.; Suzuki, A.; Asakawa, Y.; Terada, S.; Okita, M.; Fukunishi, S.; Tachikawa, T. Fabrication and characterization of  $\text{CH}_3\text{NH}_3\text{PbI}_3$  solar cells with added guanidinium and inserted with decaphenylpentasilane. *Jpn. J. Appl. Phys.* **2022**, *61*, SB1024. [[CrossRef](#)]
43. Okumura, R.; Oku, T.; Suzuki, A.; Okita, M.; Fukunishi, S.; Tachikawa, T.; Hasegawa, T. Effects of adding alkali metals and organic cations to cu-based perovskite solar cells. *Appl. Sci.* **2022**, *12*, 1710. [[CrossRef](#)]
44. Asakawa, Y.; Oku, T.; Kido, M.; Suzuki, A.; Okumura, R.; Okita, M.; Fukunishi, S.; Tachikawa, T.; Hasegawa, T. Fabrication and characterization of  $\text{SnCl}_2$ - and  $\text{CuBr}$ -added perovskite photovoltaic devices. *Technologies* **2022**, *10*, 112. [[CrossRef](#)]
45. Terada, S.; Oku, T.; Suzuki, A.; Okita, M.; Fukunishi, S.; Tachikawa, T.; Hasegawa, T. Ethylammonium bromide- and potassium-added  $\text{CH}_3\text{NH}_3\text{PbI}_3$  perovskite solar cells. *Photonics* **2022**, *9*, 791. [[CrossRef](#)]

**Disclaimer/Publisher’s Note:** The statements, opinions and data contained in all publications are solely those of the individual author(s) and contributor(s) and not of MDPI and/or the editor(s). MDPI and/or the editor(s) disclaim responsibility for any injury to people or property resulting from any ideas, methods, instructions or products referred to in the content.